Electronic structure of a Mn_6 (S=4) single molecule magnet grafted on Au(111)

U. del Pennino,[1,2] V. Corradini,[2] R. Biagi,[1,2] V. De Renzi,[1,2] F. Moro,[1,2] D. W. Boukhvalov,[3] G. Panaccione,[4] M. Hochstrasser,[4] C. Carbone,[5] C. J. Milios,[6] and E. K. Brechin[6]

[1]*INFM-S3 and Dipartimento di Fisica, Università di Modena e Reggio Emilia, 41100 Modena, Italy*

[2]*INFM National Center on nanoStructures and bioSystems at Surfaces (S3), 41100 Modena, Italy*

[3]*Institute for Molecules and Materials, Radboud University Nijmegen, NL-6525 ED Nijmegen, The Netherlands*

[4]*TASC-INFM Beamline APE, 34012 Trieste, Italy*

[5]*CNR-ISM, 34100 Trieste, Italy*

[6]*School of Chemistry, The University of Edinburgh, EH9 3JJ Edinburgh, United Kingdom*

(Received 30 July 2007; published 13 February 2008)

Single molecule magnets (SMMs) form a new class of magnetic materials consisting of identical nanoscale particles that can show magnetization in the absence of a magnetic field. We have experimentally and theoretically investigated the low-spin (S=4) member of the Mn6 SMM family, properly functionalized with two 3-thiophenecarboxylate (3tpc) ligands in order to graft it on to a Au(111) surface. We report the theoretical density of states calculated within the local density approximation (LDA) scheme accounting for the on-site Coulomb repulsion (LDA+U) for U values ranging from 0 to 8 eV. On the experimental side, by exploiting resonant photoemission at the Mn 2p edge, we were able to single out the Mn 3d derived states in the valence band energy region for a submonolayer distribution of Mn6-3tpc deposited on Au(111). From the comparison between the experimentally derived 3d density of states and the theoretical one, we found that the best agreement occurs for a U value of 4 eV. From the binding energy of Mn $2p_{3/2}$ core line, measured *in situ*, we also derived a value for the 2p-3d correlation energy of about 5 eV—in agreement with previous determination.

DOI: 10.1103/PhysRevB.77.085419 PACS number(s): 68.37.Xy, 75.50.Xx, 61.46.Bc, 73.22.−f

INTRODUCTION

Single molecule magnets (SMMs) or molecular spin clusters represent a new class of "zero-dimensional" magnetic materials consisting of almost noninteracting, identical pointlike nanoscale entities.[1–3] Below a very low temperature (blocking temperature), they can retain their magnetization in the absence of a magnetic field and so represent the smallest possible magnetic storage device. The characteristics of SMMs derive from their intrinsic properties of combining a high-spin ground state with a large and negative (easy axis type) magnetoanisotropy.[4]

Recently, a family of SMMs containing six Mn^{III} atoms has received great attention since one of its members (Mn_6O_2(Et-sao)$_6$[O_2CPh(Me)$_2$]$_2$(EtOH)$_6$) showed an effective energy barrier for magnetization relaxation of 86.4 K.[5] Actually, there are two distinct categories of molecules within this family, one with spin ground state S=4,[6] and other with S=12, which presents the high energy barrier quoted above. The "switch" from an antiferromagnetic exchange in the former class to a ferromagnetic exchange in the latter appears related to a structural distortion induced in the cluster by the presence of bulky oximato derivatives. In order to understand the basic electronic properties of this family of SMMs, we focus our attention on the electronic properties of the first member of the family, the Mn6 compounds with S=4.

The electronic properties of such SMMs can be investigated by *ab initio* calculations though if the core of a SMM contains transition metal (TM) atoms, an intrinsic difficulty is the presence of correlation effects between the 3d electrons of the TM. Various SMMs have already been investigated by *ab initio* mehods,[7–12] and we have previously carried out calculations on SMMs (accounting for the Coulomb repulsion U) by the local density approximation LDA+U method described in Ref. 13. A detailed discussion of the implementation of the LDA, generalized gradient approximation, and LDA+U methods for SMMs was outlined in Refs. 7 and 11.

One of the most relevant results of the calculations on SMMs is the total density of states (DOS), and in particular, the part associated with the TM 3d states which should be compared with those experimentally derived—typically by photoemission. In reality, it is not easy to obtain the experimental 3d DOS by standard photoemission because at low photon energies, the valence band (VB) of the compounds is dominated by the broad contributions of oxygen, carbon, and all other atoms forming the organic shell of the molecule, while at high photon energies, the overall VB cross section is quite low.[14] Furthermore, if the SMM is deposited as thin layer on a metallic surface (typically gold), the VB spectrum is dominated by the substrate (Au 5d) contribution.

One way to extract the sole contribution of the 3d derived states from the SMM VB spectra is to use resonant photoemission spectroscopy (RESPES) measured at energies corresponding to the TM $L_{2,3}$ or $M_{2,3}$ edge. In this way, only the partial DOS corresponding to Mn 3d states are set into evidence. In fact, the photoemission of d electrons from a 3d-TM is strongly enhanced when the energy of the incoming photon is able to excite a mp electron (m=2,3) to an unoccupied 3d level. This mechanism was first explained in an atomic picture by Fano[15] as a process in which a np electron excited into an empty 3d level forms a tightly bound (mp,3d) intermediate state which can decay, via autoioniza-

tion, to a final state with a hole in the filled $3d$ states. This final state is identical to that obtained via direct photoemission of a $3d$ electron, and the two emission channels can interfere quantum mechanically giving a particular shape to the absorption edge (Fano line shape). This phenomenon is more relevant for the $3p \rightarrow 3d$ transition, where the two photoemission channels have comparable intensities, and less evident at the $2p \rightarrow 3d$ edge, where the indirect channel prevails and the photoemission is particularly large (giant resonance). For Mn, for example, the $3d$ electron resonance occurs when the direct photoemission channel ($mp^6 3d^n + h\nu \rightarrow mp^6 3d^{n-1} + \varepsilon_f$) interferes with the Mn $mp \rightarrow 3d$ excitation followed by a Coster-Kronig decay, $mp^6 3d^n + h\nu \rightarrow mp^5 3d^{n+1} \rightarrow mp^6 3d^{n-1} + \varepsilon_f$. The actual value of the $3d$ occupation number n depends on the oxidation state of the TM atoms ($n=4$ in Mn6) and can have multiple values in some SMMs (e.g., Mn12, $n=3,4$).

RESPES measurements at the Mn $L_{2,3}$ edges of the prototype Mn12 SMM with different functionalizations have already enabled the extraction of the Mn partial $3d$ DOS which was found quite similar in the different compounds and satisfactorily compared with the theoretical d DOS obtained by the LDA+U method using a $U=4$ eV.[8,16]

The aim of the present study is to extend the use of resonant photoemission at the Mn $2p \rightarrow 3d$ edge, to a submonolayer distribution of functionalized Mn6 SMMs grafted on Au(111), in order to derive the experimental DOS associated with Mn $3d$ states and compare it with the corresponding DOS calculated by means of LDA+U.

The functionalized Mn6-3tpc (3-thiophenecarboxylate) derives from the complex $[Mn^{III}_6O_2(sao)_6(O_2CPh)_2(EtOH)_4]$ (where $saoH_2$=salicylaldoxime or 2-hydroxybenzaldehyde oxime=$C_7H_7NO_2$), which is characterized by an S=4 spin ground state as a result of the ferromagnetic exchange between two antiferromagnetically coupled $[Mn^{III}_3]$ triangles.[6] This compound has been functionalized with two 3-thiophenecarboxylate ligands to enable its grafting on Au(111). As the two 3tpc units have their S atoms in the outer position of the TP ring protruding from the molecular plane in opposite directions, they should force the molecules to graft onto the gold surface with their axis normal to the surface.

By exploiting RESPES, we could extract the experimental DOS associated with the Mn $3d$ electrons and compare it with that calculated by the LDA+U method; we were then able to assess that the U value providing the best agreement is 4 eV. The shape of the resonant peak is discussed in terms of occupation number in the final state.

Finally, the comparison of the photon energy corresponding to the edge of the Mn L_3 absorption and the Mn $2p_{3/2}$ binding energy suggested a $2p$-$3d$ correlation energy of about 5 eV, in agreement with previous results on analogous systems.

CALCULATIONS

Electronic structure calculations were carried out within the LDA taking into account on-site Coulomb repulsion (LDA+U).[13] We used the atomic sphere approximation linear muffin-tin orbital ASA-LMTO method[18] exploiting the Stuttgart TB-47 code. Previously, the same approach had been successfully used for the calculation of the electronic structure and exchange interactions in many molecular magnets: Mn12,[7,8] Fe8,[9] V15,[10,11] and V12.[12] Taking into account the on-site Coulomb repulsion not only gives an energy gap[11,12,17] close to experimental values but also reproduces the experimental band structure.[7–10,16] Furthermore, the exchange calculated within the LDA+U method produces the correct ground state spin[8] and magnetization curves.[11] In our previous papers,[8,12] we demonstrated a qualitative agreement between the calculated value of the on-site Coulomb repulsion and the value obtained from the comparison of the calculated energy gap and band structure with experiment. These comparisons for Mn12, V15 and Fe8, and one analog of V12 all gave a U value of 4 eV, whereas for a second analog of V12, it resulted $U \approx 6$ eV.

In Ref. 12, the influence of the geometrical structure on the electronic structure and value of U was shown. Mn6 belongs to a new family of SMMs where the Mn ions are connected not only via oxygen atoms but also via -N-O-bridges (via Et-sao^{2-} ligands). Present calculations were carried out for the full structure of Mn6 without omitting any part of the molecule or solvent. The radii of the MT spheres of Mn, O, N, C, and H used in the calculation are about 2.6, 1.9, 1.5, 1.4, and 1.0 a.u., respectively. To complete the cell, 41 empty spheres per Mn molecule were added. The calculation was performed for eight k points in the irreducible part of the Brillouin zone. Further detail was common to any other calculation of the electronic structure within the ASA-LMTO method. We performed different calculations within the standard LDA functional and by adding on-site Coulomb repulsion with values of U from 2 to 8 eV in steps of 2 eV for Mn. All densities of states were smeared by Gaussians of 0.2 eV half width at half maximum.

EXPERIMENT

The Mn6-3tpc compound (shown in Fig. 1) was obtained by the reaction of $Mn(ClO_4)_2 \cdot 6H_2O$ with $saoH_2$ (salicylaldoxime), 3-thiophene carboxylic acid, and NaOMe in MeOH. The green-black crystalline sample was isolated after slow evaporation of the bulk solution. The substrates were flame annealed Au(111) thick films deposited on mica or highly oriented pyrolitic graphite slabs. The SMM submonolayer was deposited on the Au substrate by dipping it in a 1 mM solution of Mn6-3tpc in dichloromethane (CH_2Cl_2), while SMM thick films were obtained by drop casting the solution on graphite.

The deposition process was monitored *on campus* by means of scanning electron microscopy (STM) and x-ray photoemission spectroscopy (XPS) measurements. STM images were acquired by an Omicron VT-STM at room temperature. Typical imaging conditions were a bias voltage of 2.0 V and a tunneling current of 30 pA, in order to minimize dragging and damaging of the soft organic materials with the STM tip.

Nonmonochromatized x rays from an Al anode were used to excite the spectra of the main elements in Mn6-3tpc. Pho-

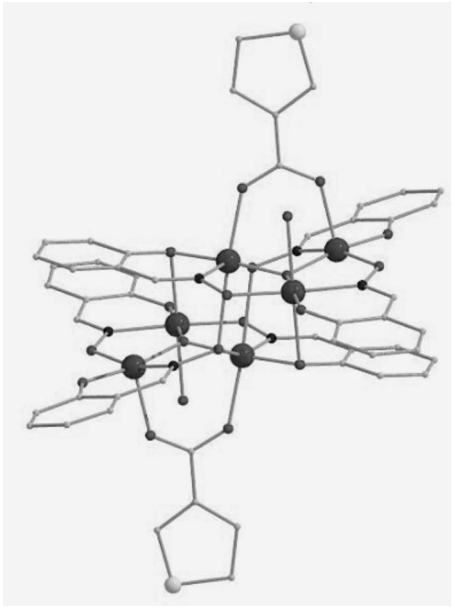

FIG. 1. The molecular structure of the Mn6-3tpc derivative with the two 3tpc ligands protruding in opposite directions normally to the molecular plane. Large dark balls: Mn; smaller dark balls: O; and large gray balls: S.

toemitted electrons were analyzed by means of an Omicron EA 125 mm, seven channeltrons, hemispherical analyzer, with a total energy resolution of 1.4 eV.

X-ray absorption spectroscopy (XAS) and RESPES measurements were carried out at the APE beamline of the ELETTRA synchrotron radiation laboratory in Trieste, Italy. The variable-polarization–high energy undulator emits in the soft x-ray range (200–2000 eV) with a photon flux of the order of 10^{12} ph/s on the sample, within 0.01% bandwidth. The monochromator resolving power $E/\Delta E=5\times10^3$.

The x-ray absorption spectra were obtained by measuring the total electron yield and normalizing it to the monitor current. The RESPES measurements exploited an Omicron EA 125 mm, seven channeltrons, hemispherical analyzer, with a total energy resolution of 0.35 eV. Setting the photon energy to 1400 eV, it was also possible to record on the beamline some x-ray photoelectron spectra to measure the actual binding energy of Mn in the same compounds and in the same conditions of the x-ray absorption spectra.

RESULTS AND DISCUSSION

The deposition of Mn6-3tpc was monitored by STM and XPS. The RT STM image reported in Fig. 2 (right panel) shows the presence of a quite homogeneous two-dimensional distribution of isolated Mn6 clusters with no evidence of three-dimensional aggregates (higher than 20 Å) and a low number of two-dimensional (2D) aggregates with diameter larger than 50 Å. The stability of the clusters even at higher tunneling currents (not shifted by the scanning tip) confirms the strength of the molecular bond with the Au surface.

From the STM line profile of a single entity [Fig. 2 (left panel)], we derived a diameter of 3.5 ± 0.5 nm and height of 0.8 ± 0.2 nm, in agreement with the expected dimensions of the functionalized cluster, assuming the orientation of the ring axis normal to the surface (1.8 nm and 1.5 nm respectively), once convoluted with the curvature radius of the tip which is not negligible. From a statistical analysis of the STM images, we derived that approximately 18%–25% of the surface is occupied by the 2D distribution of clusters.

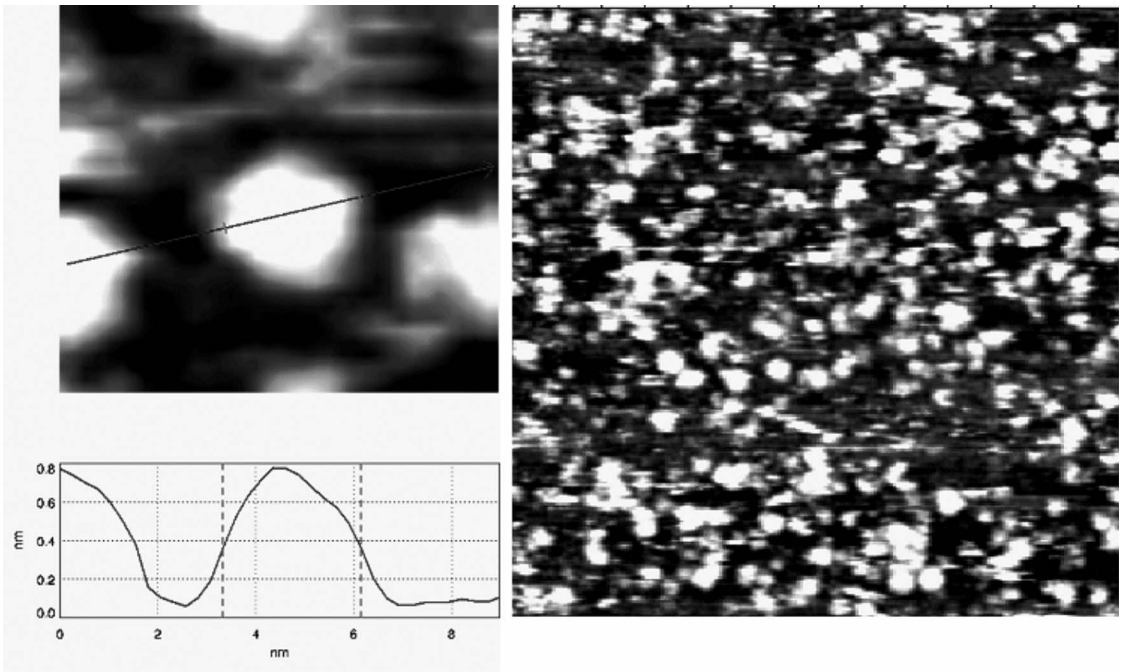

FIG. 2. Right panel: constant-current (30 pA, 2 V) STM image of 70×70 nm^2. The white entities represent the clusters of Mn6-3tpc grafted onto Au(111) surface. Left panel: STM height profile of a single Mn6-3tpc cluster.

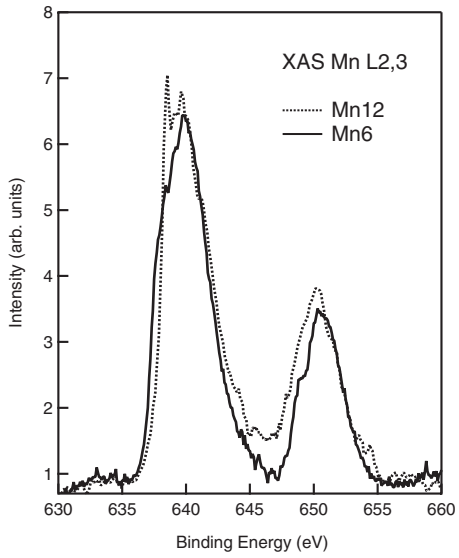

FIG. 3. Mn $L_{2,3}$ edge x-ray absorption spectrum for a ML of Mn6-3tpc on Au(111) (solid line) compared with the corresponding spectrum for a Mn12Ac ML taken from Ref. 8 (dotted line).

The corresponding XPS investigation of the monolayer (ML) confirmed the coverage derived from STM, and the comparison with the stoichiometry of the thick layer confirms the integrity of the Mn6-3tpc core in the ML. The energy positions of the S $2p$ core level (about 162.5 eV) clearly indicates the presence of a strong S–Au bond confirming the cluster stability observed in the STM images.

As a first step in the resonant photoemission investigation of Mn6-3tpc, we measured the Mn $L_{2,3}$ edge x-ray absorption spectrum in the photon energy range spanning the $L_{2,3}$ $(2p)$ edge of Mn (630–665 eV). The XAS spectra taken on the submonolayer coverage and on the thick film do not show significant differences, confirming again that the electronic properties of the Mn6 core are preserved in the deposition process. The XAS curve for the Mn6-3tpc ML, after a spline background subtraction, is shown as solid line in Fig. 3 together with the corresponding spectrum for the Mn12Ac ML taken from Ref. 8 (dotted line), shifted by 1.5 eV toward lower photon energy. The absence, in the whole set of measurements, of the peak at lower photon energy (approximately 638 eV) due to the presence of reduced (Mn^{2+}) species evidences the greater redox stability of the submonolayer of Mn6-3tpc as compared to the Mn12 derivatives.

The XPS measurements carried out on the same samples at the synchrotron beamline showed a Mn $2p_{3/2}$ core level binding energy of 642.3 eV, a typical value for Mn oxides. However, the onset of the XAS curve corresponding to the transition from the filled $2p_{3/2}$ to the empty part of the $3d$ can be set at about 636 eV (see Fig. 3), 6.3 eV lower than that expected on the basis of a naive single particle approach. Therefore, accounting for a gap of about 1.5 eV (as indicated by calculations, shown below), these results seem to indicate a $2p$-$3d$ correlation energy of about 5 eV, which reduces the measured energy of the $2p \rightarrow 3d$ transition. A value of 5 eV for the Mn $2p$-$3d$ correlation energy had already been found in MnTe.[19]

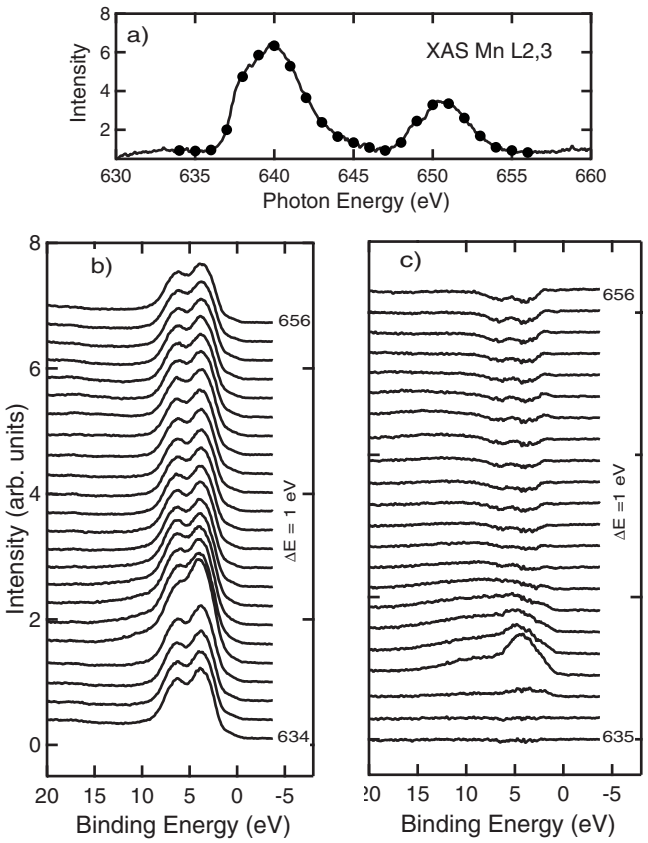

FIG. 4. Panel (a): Mn6-3tpc/Au(111) VB spectra at increasing photon energies across the Mn $L_{2,3}$ edge. The corresponding measurement energies are indicated by black dots superimposed on the absorption spectrum in the inset. Panel (b): difference between spectra in panel (a) (for $h\nu \geqslant 635$ eV) and spectrum at $h\nu = 634$ eV.

Once acquired the absorption spectra, we could identify the energies at which to carry out the photoemission measurements. These are indicated by the black dots superimposed on the absorption spectrum in the inset of Fig. 4(a), which reports the Mn6-3tpc VB spectra at increasing photon energies from 634 to 656 eV in 1 eV steps.

As the Mn6 molecules cover only 20% of the substrate, the main contribution to the spectra comes from the Au VB states, and some enhancement can be clearly detected only for $h\nu = 638$ eV. Therefore, to be able to better single out the enhancement corresponding to the Mn $3d$ DOS at all the measured energies, we subtracted (at each VB spectrum) the first one (off-resonance spectrum) measured at $h\nu = 634$ eV. The difference spectra are shown in Fig. 4(b) where different spectra show an enhancement around the L_3 edge. This last figure deserves two further comments. We see in fact that (i) no clear resonance appears at the L_2 edge and (ii) no Auger signal is detected in the spectra. These two characteristics seem to be common to all the SMM monolayers we investigated: Mn6, Mn12Ac,[8] and Cr_7Ni.[20] The delayed onset of the Auger signal could be due to a negligible delocalization of the intermediate state in the noninteracting clusters.[21] By the way, we notice that the Auger signal is perfectly detectable in a Cr_7Ni thick layer.[20] The very low intensity (if any) of the

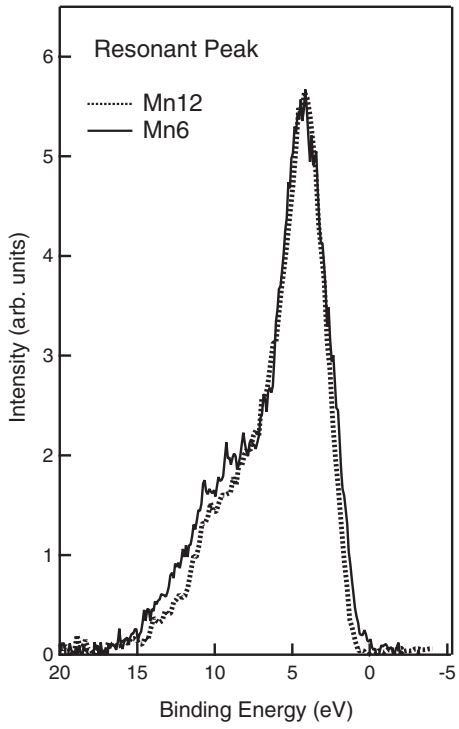

FIG. 5. Difference between the on resonance ($h\nu$=638 eV) and the off-resonance ($h\nu$=634 eV) spectra for Mn6-3tpc ML showing the Mn 3*d* contribution to the VB (solid line) compared with the corresponding curve for Mn12Ac ML taken from Ref. 8 (dotted line).

L_2 resonance must be checked and investigated in more detail. Finally, the "negative feature" appearing at increasing photon energies in the BE range of 3–9 eV is just the effect of the decreasing photoemission cross section of the Au substrate (as directly measured on a clean sample).

In Fig. 5, we show the spectrum showing the strongest resonance at $h\nu$=638 eV (solid line), together with the corresponding 3*d* DOS obtained in similar conditions for a ML of Mn12/Au (dotted line), taken from Ref. 8. The two spectra are very similar, though the Mn atoms in Mn6 and in Mn12 have different oxidation states. Furthermore, the spectral shape is also quite similar to that obtained by the same method for MnTe (Ref. 19) and MnO.[21] The explanation (in an atomistic picture) can be that, due to correlation effects among the 3*d* electrons, the energy of the photoemission final state changes drastically with the number of electrons in the 3*d* state, *n*. For Mn^{III}, therefore, the photoemission final state at higher energy is $3d^3$, present in all the cited compounds, and its shape depends only marginally on the environment. On the other hand, the $3d^2$ final state (like in Mn12) with a higher number of holes lies much deeper in energy and probably with lower intensity, and it does not appear in the VB spectra.

In Fig. 6, we show the results of the calculations by LDA+*U* of the electronic structure of 3tpc Mn6 by reporting the 3*d* derived DOS for different values of the Coulomb repulsion *U*. It is evident that for *U* below 4 eV, the system is still metallic and that a gap (of about 1.5 eV) opens only for $U \geqslant 4$ eV. For these last values of *U*, the theoretical DOS

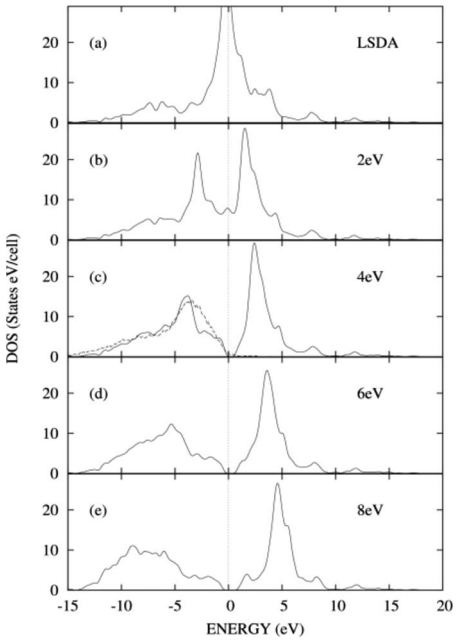

FIG. 6. Partial DOS for 3*d* orbitals of Mn obtained by the (a) LSDA and [(b)–(e)] LDA+*U* method using a *U* value from 2 to 8 eV. Dashed line on panel c corresponds to the experimental spectrum in Fig. 5.

has been compared with the experimental spectrum shown in Fig. 5. The calculated DOS whose bandwidth, shape, and energy position of the maximum result in best agreement with the experimental spectrum is that corresponding to *U* =4 eV. The experimental spectrum (drawn as a dashed line) has been superimposed on the theoretical curve in Fig. 6 (panel c). This spectrum has been slightly shifted in energy and normalized in height to get the best agreement with the calculated DOS in the region below −4 eV. The experimental and theoretical bandwidths coincide and the overall shapes are quite similar. In both cases, two features are also evident at approximately −4 and −9 eV of BE. Only the region between −1 and −3 eV in the theoretical DOS results in numbers lower than the experimental data. There can be different reasons why a photoemission spectrum cannot exactly reproduce the theoretical DOS: besides the effects of the matrix elements, the spectrum corresponds to a final state with $n-1$ electrons, whereas the one obtained theoretically is a *n*-electron state.

With this caveat in mind, it is interesting to note that the experimentally derived 3*d* DOS for the compounds quoted in Refs. 19 and 21 in the BE region of 0–3 eV agrees with the theoretical one better than our spectrum. As in the present case, the Mn6 molecules are grafted on Au, and we could suppose that the extra-3*d* states near the top of the VB populated in grafted Mn6 arise from the bonding to Au, though a charge transfer from the Au substrate to the sulfur atom is not expected to be high[22] and the Mn atoms are spatially well separated from the substrate.

CONCLUSIONS

We investigated both experimentally and theoretically the low-spin (S=4) member of the Mn6 SMM family function-

alized with 3-thiophenecarboxylate and grafted on Au(111). We showed that also in the case of functionalized Mn6, the LDA+U approach is able to give reliable density of states and reported those corresponding to U values between 0 and 8 eV. On the experimental side, we measured the x-ray absorption spectrum of Mn6-3tpc at the Mn $L_{2,3}$ edge and by exploiting resonant photoemission at the L_3 edge, we were able to single out the Mn 3d derived states in the VB of the submonolayer of Mn6-3tpc deposited on Au(111).

By measuring *in the same apparatus* the XAS and XPS of a SMM, we could derive from the values of the Mn L_3 absorption edge and of the Mn $2p_{3/2}$ binding energy the value of the 2p-3d correlation energy, about 5 eV, in agreement with the value previously found for MnTe. From the comparison between the experimentally derived and theoretical 3d DOS, we found that the best agreement occurs for a U value of 4 eV, in which case the two bandwidths coincide, the overall shapes are quite similar and two features are also evident in both DOS at approximately −4 and −9 eV of BE. This ample agreement suggests that the effect of the 2p hole on the 3d DOS line shape, not accounted for in the calculations, could be not so strong as expected.

On the other hand, a comparison with the corresponding experimental DOS's for different Mn compounds present in the literature suggests that their shape corresponds to the $3d^3$ final state, scarcely depending on the environment of the Mn atoms. A further new result specific to a SMM monolayer grafted on a metal is that the resonance at the L_2 is negligible and the Auger emission is largely delayed with respect to the L_3 edge, indicating a strong localization of the intermediate state in the noninteracting single clusters.

ACKNOWLEDGMENTS

This work was financially supported by the EC Network of Excellence MAGMANet (N.515767). D. W. Boukhvalov acknowledges support from Stichting voor Fundamenteel Onderzoek der Materie (FOM), Netherlands.

[1] O. Kahn, *Molecular Magnetism* (VCH, New York, 1993).
[2] *Molecular Magnets: From Molecular Assemblies to the Devices*, edited by E. Coronado, P. Delhaès, D. Gatteschi, and J. S. Miller (Kluwer, Dordrecht, 1996).
[3] D. Gatteschi, A. Caneschi, L. Pardi, and R. Sessoli, Science **265**, 1054 (1994).
[4] G. Christou, D. Gatteschi, D. N. Hendrickson, and R. Sessoli, MRS Bull. **25**, 66. (2000).
[5] C. J. Milios, A. Vinslava, P. A. Wood, S. Parsons, W. Wernsdorfer,G. Christou, S. P. Perlepes, and E. K. Brechin, J. Am. Chem. Soc. **129**, 2754 (2007).
[6] C. J. Milios, C. P. Raptopoulou, A. Terzis, F. Lloret, R. Vicente, S. P. Perlepes, and A. Escuer, Angew. Chem., Int. Ed. **43**, 210 (2004).
[7] D. W. Boukhvalov, M. Al-Saqer, E. Z. Kurmaev, A. Moewes, V. R. Galakhov, L. D. Finkelstein, S. Chiuzbaian, M. Neumann, V. V. Dobrovitski, M. I. Katsnelson, A. I. Lichtenstein, B. N. Harmon, K. Endo, J. M. North, and N. S. Dalal, Phys. Rev. B **75**, 014419 (2007).
[8] U. del Pennino, V. De Renzi, R. Biagi, V. Corradini, L. Zobbi, A. Cornia, D. Gatteschi, F. Bondino, E. Magnano, M. Zangrando, M. Zacchigna, A. Lichtenstein, and D. W. Boukhvalov, Surf. Sci. **600**, 4185 (2006).
[9] D. W. Boukhvalov, E. Z. Kurmaev, A. Moewes, D. A. Zatsepin, V. M. Cherkashenko, S. N. Nemnonov, L. D. Finkelstein, Yu. M. Yarmoshenko, M. Neumann, V. V. Dobrovitski, M. I. Katsnelson, A. I. Lichtenstein, B. N. Harmon, and P. Kogerler, Phys. Rev. B **67**, 134408 (2003).
[10] D. W. Boukhvalov, E. Z. Kurmaev, A. Moewes, M. V. Yablonskih, S. Chiuzbaian, L. D. Finkelstein, M. Neuman, M. I. Katsnelson, V. V. Dobrovitski, and A. I. Lichtenstein, J. Electron Spectrosc. Relat. Phenom. **137–140**, 735 (2004).
[11] D. W. Boukhvalov, V. V. Dobrovitski, M. I. Katsnelson, A. I. Lichtenstein, B. N. Harmon, and P. Kogerler, Phys. Rev. B **70**, 054417 (2004).
[12] A. Barbour, R. D. Luttrell, J. Choi, J. L. Musfeldt, D. Zipse, N. S. Dalal, D. W. Boukhvalov, V. V. Dobrovitski, M. I. Katsnelson, A. I. Lichtenstein, B. N. Harmon, and P. Kögerler, Phys. Rev. B **74**, 014411 (2006).
[13] V. I. Anisimov, F. Aryasetiawan, and A. I. Lichtenstein, J. Phys.: Condens. Matter **9**, 767 (1997).
[14] J.-S. Kang, J. H. Kim, Yoo Jin Kim, Won Suk Jeon, Duk-Young Jung, S. W. Han, K. H. Kim, K. J. Kim, and B. S. Kim, J. Korean Phys. Soc. **40**, L402 (2002).
[15] U. Fano, Phys. Rev. **124**, 186 (1961).
[16] S. Voss, M. Fonin, U. Rüdiger, M. Burgert, U. Groth, and Yu. S. Dedkov, Phys. Rev. B **75**, 045102 (2007).
[17] S. Voss, M. Fonin, U. Rüdiger, M. Burgert, and U. Groth, Appl. Phys. Lett. **90**, 133104 (2007).
[18] O. K. Andersen, Phys. Rev. B **12**, 3060 (1975).
[19] H. Sato, A. Tanaka, A. Furuta, S. Senba, H. Okuda, K. Mimura, M. Nakatake, Y. Ueda, M. Tanigichi, and T. Jo, J. Phys. Soc. Jpn. **68**, 2132 (1999).
[20] R. Biagi, V. Corradini, V. De Renzi, F. Moro, U. del Pennino, V. Bellini, D. Tomecka, G. A. Timco, R. E. P. Winpenny, M. Hochstrasser, and G. Panaccione, (unpublished).
[21] M. C. Richter, J.-M. Mariot, O. Heckmann, L. Kjeldgaard, B. S. Mun, C. S. Fadley, and K. Hricovini, Nucl. Instrum. Methods Phys. Res. B **246**, 184 (2006).
[22] V. De Renzi, R. Rousseau, D. Marchetto, R. Biagi, S. Scandolo, and U. del Pennino, Phys. Rev. Lett. **95**, 046804 (2005).